Preparation, Structure, and Properties of Three-Dimensional Ordered α-Fe_2O_3 Nanoparticulate Film

Lihua Huo,[†,‡] Wei Li,[†] Lehui Lu,[†] Haining Cui,[†] Shiquan Xi,*[,†] Jing Wang,[§] Bing Zhao,[§] Yaochun Shen,[§] and Zuhong Lu[§]

Laboratory of Rare Earth Chemistry and Physics, Changchun Institute of Applied Chemistry, Chinese Academy of Sciences, Changchun 130022, China, College of Chemistry and Chemical Technology, Heilongjiang University, Harbin 150080, China, and National Laboratory of Molecular & Biomolecular Electronics, Southeast University, Nanjing 210096, China

Received October 28, 1999

α-Fe_2O_3 nanoparticulate films could be formed on the surface of α-Fe_2O_3 hydrosol after aging of the hydrosol or by compressing of the nanoparticles on the sol surface, in which a three-dimensional ordered structure was constructed by the Langmuir−Blodgett technique and colloid chemical methods. The structure of the LB film was characterized by AFM, TEM, XPS, and UV−vis spectra and small-angle X-ray diffraction. Gas-sensing measurement shows that the LB film has good sensitivity to alcohols at room temperature.

Introduction

Over the past two decades, nanosized inorganic semiconductor particles have become an important subject of increasing interest in material science research and development, owing to their unusual chemical and physical properties. Their thin films have shown to have potential applications in multifunctional microelectronic and molecular devices.[1−4] Therefore, organized assemblies of nanoparticles in two or even three dimensions have attracted much attention in recent years.[5]

Ferric oxide is a conventional semiconductor material, which has been widely applied as a pigment or magnetic, nonlinear optical, and gas-sensing materials. A variety of physical and chemical methods, such as cathodic sputtering, chemical vapor deposition, spin-coating, etc., have been used to prepare Fe_2O_3 thin films.[6−8] However, these methods could barely control the nanoparticle crystal size and film thickness. The Langmuir−Blodgett technique has been used to fabricate highly ordered molecular assemblies with controlled thickness in the order of nanometers. Up to now, inorganic nanoparticulate LB films have been prepared by two assembly methods: (1) nanoparticles are covered

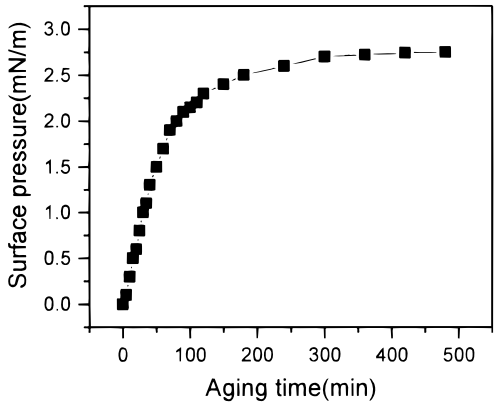

Figure 1. Surface pressure−aging time ($\pi-t$) isotherm of Fe_2O_3 hydrosol.

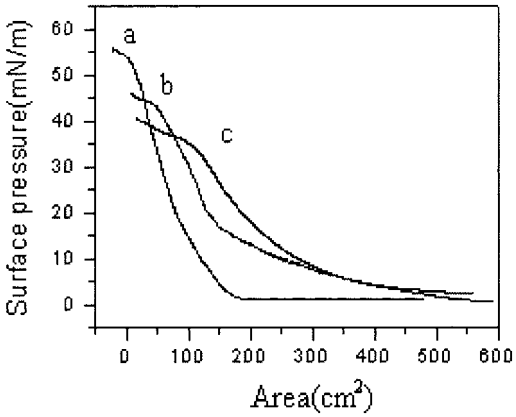

Figure 2. Surface pressure−trough area ($\pi-A$) isotherm on the surface of Fe_2O_3 hydrosol at different aging time (a, 0 h; b, 3 h; c, 8 h).

* Corresponding author. Fax: +86-431-5685653; E-mail: xisq@public.cc.jl.cn.
† Chinese Academy of Sciences.
‡ Heilongjiang University.
§ Southeast University.

(1) Yonezama, T.; Matsune, H.; Kunitake, T. *Chem. Mater.* **1999**, *11*, 33.
(2) Price, L. S.; Pakin, I. P.; Hardy, A. M. E.; Clark, R. J. H.; Hibbert, T. G.; Molloy, K. C. *Chem. Mater.* **1999**, *11*, 1792.
(3) Golego, N.; Studenikin, S. A.; Cocivera, M. *Chem. Mater.* **1998**, *10*, 2000.
(4) Vinodgopal, K.; Bedja, I.; Kamat, P. V. *Chem. Mater.* **1996**, *8*, 2180.
(5) Fendler, J. H.; Meldrum, F. C. *Adv. Mater.* **1995**, *7*, 607.
(6) Siroky, K.; Jiresova, J.; Hudec, L. *Thin Solid Films* **1994**, *245*, 211.
(7) Poghossian, A. S.; Abovian, H. V.; Aroutiounian, V. M. *Sens. Actuators, B* **1994**, *18−19*, 155.
(8) Cai, S. Y.; Zheng, M. S.; Jin, Z. H.; Wu, H. J. *Thin Film Sci. Technol.* **1995**, *18*, 56.

10.1021/cm990690+ CCC: $19.00
Published on Web 03/20/2000

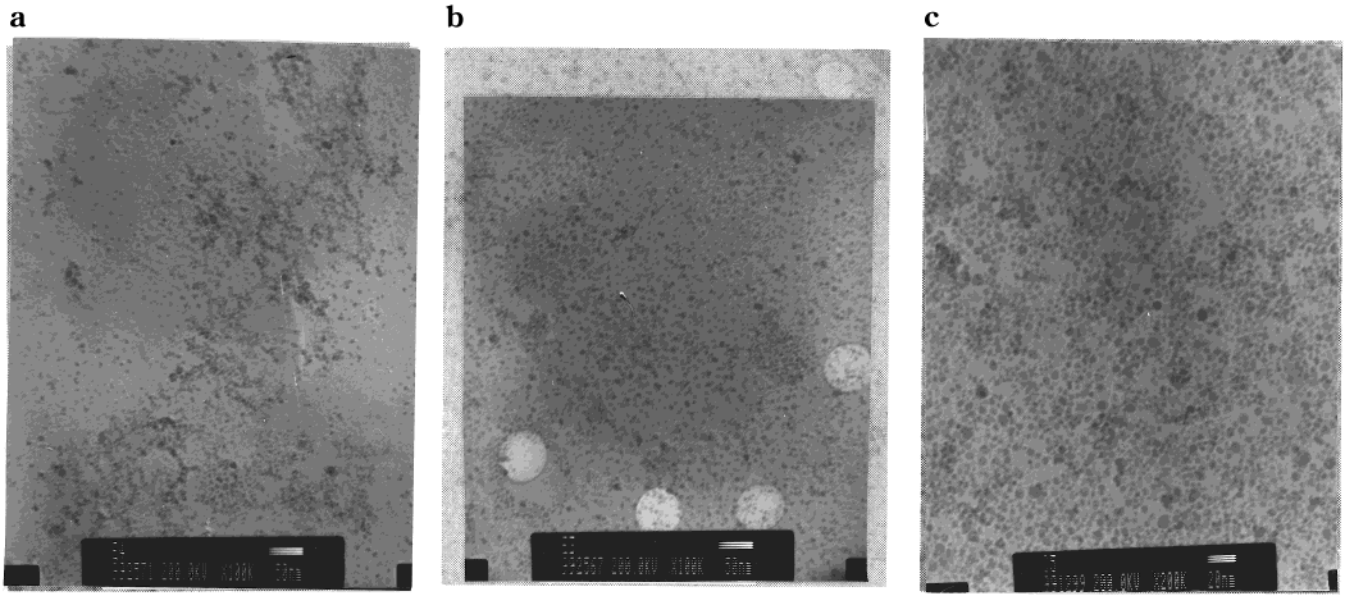

Figure 3. TEM images of Fe_2O_3 nanoparticulate monolayers on a copper grid coated with PVF (film was aged for 1 h (a) and 8 h (b); and compressed LB film (c) was deposited at 20 mN m^{-1}).

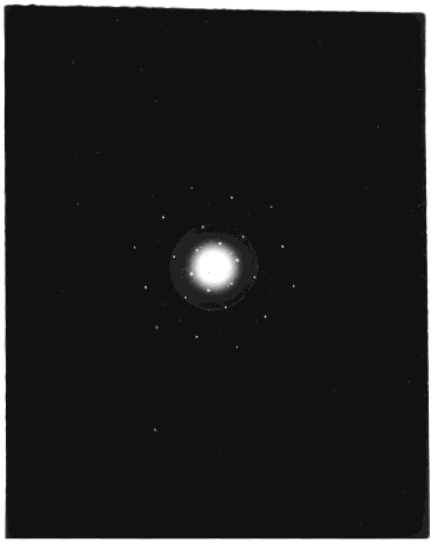

Figure 4. Electron diffraction image of Fe_2O_3 nanoparticle.

with some amphiphilic molecules[9,10] and (2) alternating multilayer nanoparticles/amphiphilic molecules LB films[11,12] are prepared using nanoparticulate hydrosol as the subphase. A pure nanoparticulate LB film has been obtained by thermodesorption of the composite LB film.[13]

Recently, a SnO_2 nanoparticulate film was obtained using the LB deposition technique.[14] As a part of inorganic nanoparticle assembly work, a α-Fe_2O_3 nanoparticulate LB film with a three-dimensional ordered structure was prepared. In this paper, we describe preparation, structure, and characterization of α-Fe_2O_3 nanoparticulate LB film.

Experimental Section

Materials. $FeCl_3 \cdot 6H_2O$ (A.R.) dissolved in deionized water (ρ >15 MΩ cm^{-1}) served as stock solution; $[Fe^{3+}] = 0.2$ mol dm^{-3}. Quartz and glass were used respectively as the substrates for UV−vis spectra and gas sensitivity determination. Quartz was rendered hydrophilic by treating sequentially with $CHCl_3$, C_2H_5OH, and pure H_2O, each for 20 min under action of ultrasonic wave. The glass, coated with 50 pairs of finger-shaped aluminum electrodes having a width of 50 μm, spaced 50 μm from the adjacent electrode, was pretreated in boiling isopropyl alcohol at least for 24 h.

Preparation of Nanoparticulate α-Fe_2O_3 Hydrosol. A total of 5 mL of stock solution was poured into a beaker containing 175 mL of deionized water under vigorous stirring, and then kept slightly boiling for 2 h. After quenching to room temperature, the solution was dialyzed against deionized water until free Fe^{3+} could not be detected. The resulting orange-red solution was the α-Fe_2O_3 nanoparticulate hydrosol (pH = 3.1). The Fe_2O_3 concentration was 1.6×10^{-3} mol dm^{-3} determined by POEMS-I type inductively coupled plasma−atomic emission spectrometer (ICP-AES) from Thermo Jarrell Ash Co. TEM shows the nanoparticles in the hydrosol are relatively homogeneous. The particle size of α-Fe_2O_3 nanoparticles is about 5−7 nm with an average size of 6.2 nm.

Fabrication of α-Fe_2O_3 Nanoparticulate Film. α-Fe_2O_3 hydrosol was put into a NIMA-622 LB trough from England. The sol surface was cleaned by a vacuum pump to pump out the old surface of the sol, revealing a fresh air−hydrosol interface. After aging for several hours, the surface pressure reached a a constant value, and a particulate film was formed. It was transferred onto substrates by horizontal dipping technique. This is the aged particulate film.

After the surface of the fresh hydrosol was aged for 3 h, the particulate film formed on the sol surface was compressed at the speed of 15 cm^2 min^{-1} to a certain surface pressure, and then transferred onto the substrate by vertical dipping technique. The dipping speed was 10 mm min^{-1}. Drying times between subsequent dips were 30 min in order to obtain good multilayers. Transfer ratio of multilayer deposition is in the range of 0.91−1.02. This is the compressed LB film.

All the fabrication experiments of nanoparticulate films were processed at temperature of 18 ± 1 °C.

(9) Meldrum, F. C.; Kotov, N. A.; Fendler, J. H. *J. Phys. Chem.* **1994**, *98*, 4506.
(10) Yang, J.; Peng, X. G.; Li, T. J.; Pan, S. F. *Thin Solid Films* **1994**, *243*, 643.
(11) Zhang, J.; Wang, D. J.; Chen, Y. M.; Li, T. J.; Mao, H. F.; Tian, H. J.; Zhou, Q. F.; Xu, H. J. *Thin Solid Films* **1997**, *300*, 208.
(12) Cao, L. X.; Huo, L. H.; Ping, G. C.; Wang, D. M.; Zeng, G. F.; Xi, S. Q. *Thin Solid Films* **1999**, *347*, 258.
(13) Brandl, D.; Schoppmann, Ch.; Tomaschko, Ch.; Markl, J.; Voit, H. *Thin Solid Films* **1994**, *249*, 113.
(14) Cao, L. X.; Wan, H. B.; Yuan, X. D.; Zeng, G. F.; Xi, S. Q. *Chin. J. Chem. Phys.* **1999**, *12* (2), 191.

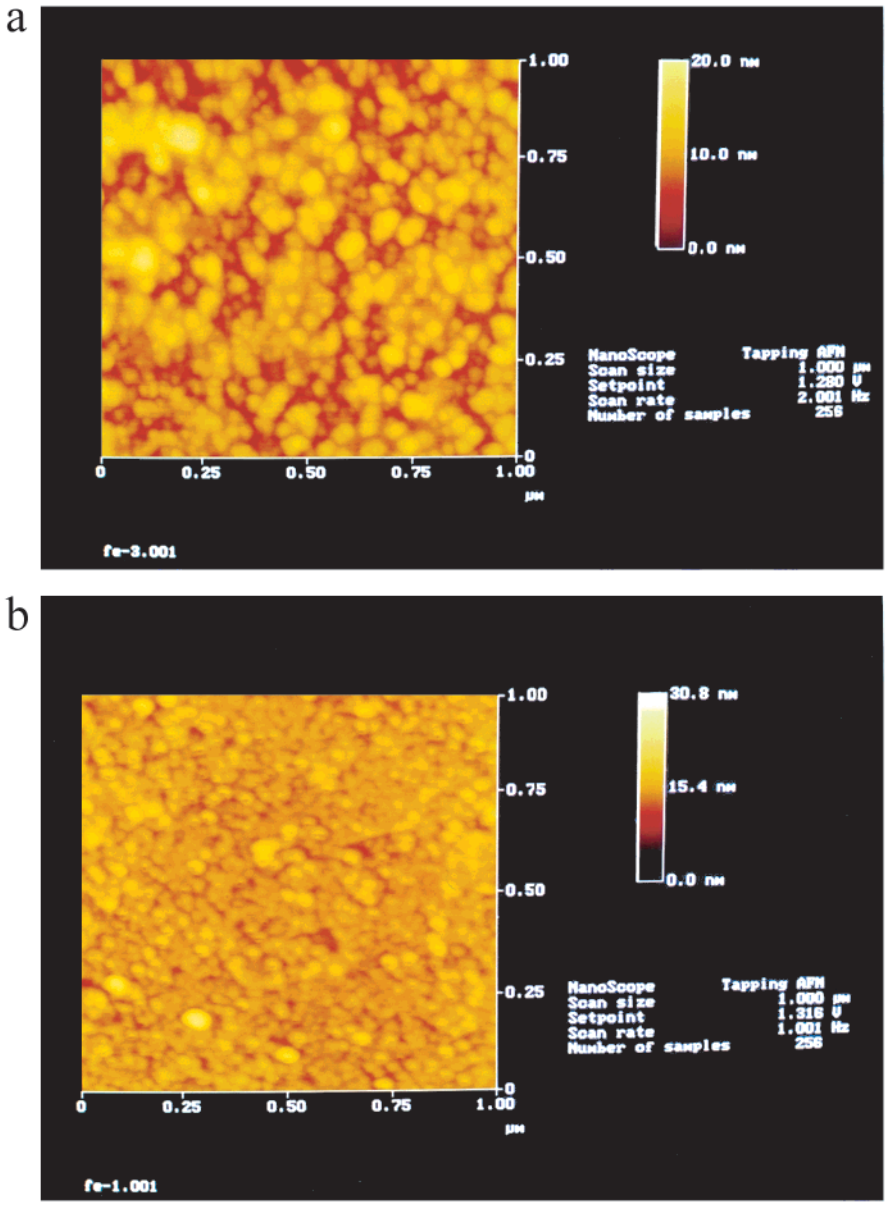

Figure 5. AFM photographs of Fe_2O_3 nanoparticulate monolayer deposited at different surface pressures on mica substrate after aging of the sol for 3 h (a, 20 mN m^{-1}; b, 30 mN m^{-1}).

Characterization of α-Fe_2O_3 Nanoparticulate Film. Electron microscopy was performed with a JEOL-2100 transmission electron microscope using 230-mesh, PVF-covered copper grids as the substrate. Tapping-mode atomic force microscopy was investigated by using a Digital Instrument of Multi-Mode AFM microscope, with mica as the substrate. Visible spectra of the film were recorded on Perkin-Elmer Lambda 9 spectrophotometer. XPS spectra were carried out using VG ESCALAB MK-II X-ray photoelectron spectrometer with Al Kα radiation ($h\nu = 1486.6$ eV). The standard deviation for the binding energy values was 0.2 eV. Small-angle X-ray diffraction pattern was measured by a Rigaku D/Max-rA diffractometer with Cu Kα. The incident X-ray beam was normal to the surface of the film.

The electrical resistance of the LB film under various gas concentrations at ambient temperature was measured with a ZCG 17 B-type 10^{17} Ω high resistance meter from China. Air was used as the diluent gas. Some amounts of alcohol were injected into a container (1000 mL) by a microsyringe and gasified at 85 °C. After the resistance of the film reached a constant value in air, the film was immediately put into the container with the desired gas concentration. The sensitivity (S) is defined as $S = R_a/R_g$, where R_a and R_g are the resistance of LB film measured respectively in air and air containing the tested gas. The response−recovery time is monitored as 90% of resistance change.

Results and Discussion

***π-t* and *π*−*A* Isotherms.** The surface of the Fe_2O_3 hydrosol was scraped clean. The initial surface pressure was defined as zero. Surface pressure was then recorded with the aging time. The relative *π-t* curve is shown in Figure 1. The surface pressure increased quickly as the aging time increased within 120 min, indicating that the fresh hydrosol was in an unstable state. The pressure then gradually approached a constant value, about 2.7 mN m^{-1}. This is a process of the nanoparticles dispersing from the bulk phase to the air−sol interface, until the interface becomes saturated, which is a process of spontaneous formation of the nanoparticulate film.

Figure 2 is the surface pressure−area (*π*−*A*) isotherms of Fe_2O_3 hydrosol at different aging time. The behavior of nanoparticulate film on the air−sol interface

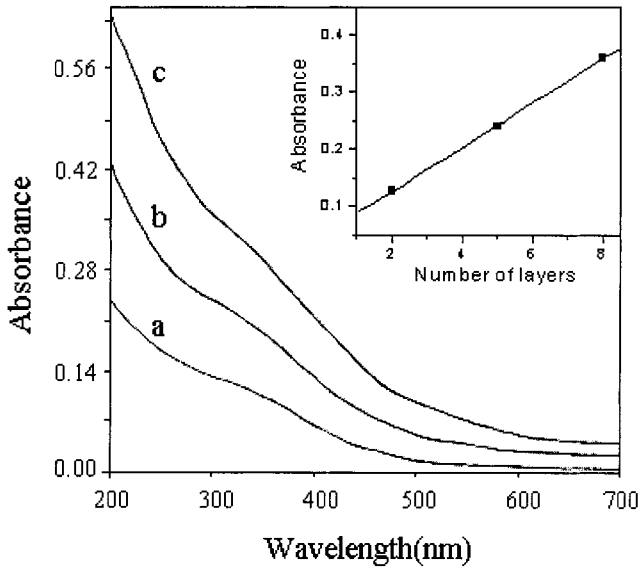

Figure 6. UV−vis spectra of 2, 5, 8 layers LB films deposited on quartz substrates at 30 mN m^{-1} (a, 2-layer; b, 5-layer; c, 8-layer; insert, absorbance vs number of layers at 300 nm).

is similar to those of the amphiphilic molecules on the pure water surface. It suggests that this kind of nanoparticulate film can be transferred onto the substrates by LB technique. Aging time has an influence on the film behavior. As the aging time increases, the phase transition point moves forward and the collapse pressure is lowered. It is related to formation of the nanoparticulate film after aging of the sol.

TEM and AFM of the Nanoparticulate Films. Figure 3 a,b shows TEM images of Fe_2O_3 nanoparticles aged for different times on the surface of the sol. For the particulate film obtained from short aging time (Figure 3a), the arrangement of the nanoparticles is inhomogeneous and some of the particles appear in aggregation. When the aging time increased, the particles arranged more homogeneously. This is related to the particles dispersing from the bulk phase to the air−sol interface. The selected area electron diffraction image (Figure 4) gives clear diffraction spots, indicating that the Fe_2O_3 particles are all well crystallized. The following XPS results demonstrate that ferric oxide nanoparticles exist as α-Fe_2O_3 phase. In comparison with TEM image of the compressed film shown in Figure 3c, the nanoparticles in the compressed film are packed more closely and homogeneously than those in the aged films.

AFM photographs of Fe_2O_3 nanoparticulate monolayers deposited onto mica substrates at surface pressure of 20 and 30mN m^{-1} are given in Figure 5. The nanoparticles are packed more closely and homogeneously with the increase in surface pressure. The higher the pressure is, the closer the particles arrange, and the fewer defects there are. The particle size observed from AFM is larger than that from TEM, resulting from the size and shape of the tip used in AFM measurement. As the nanoparticles in the compressed film are packed more closely, the samples used for structural characterization are all the compressed ones.

UV−Vis Spectra. The absorption spectra of different Fe_2O_3 nanoparticulate films on quartz deposited at 30mN m^{-1} are shown in Figure 6. The absorption onset

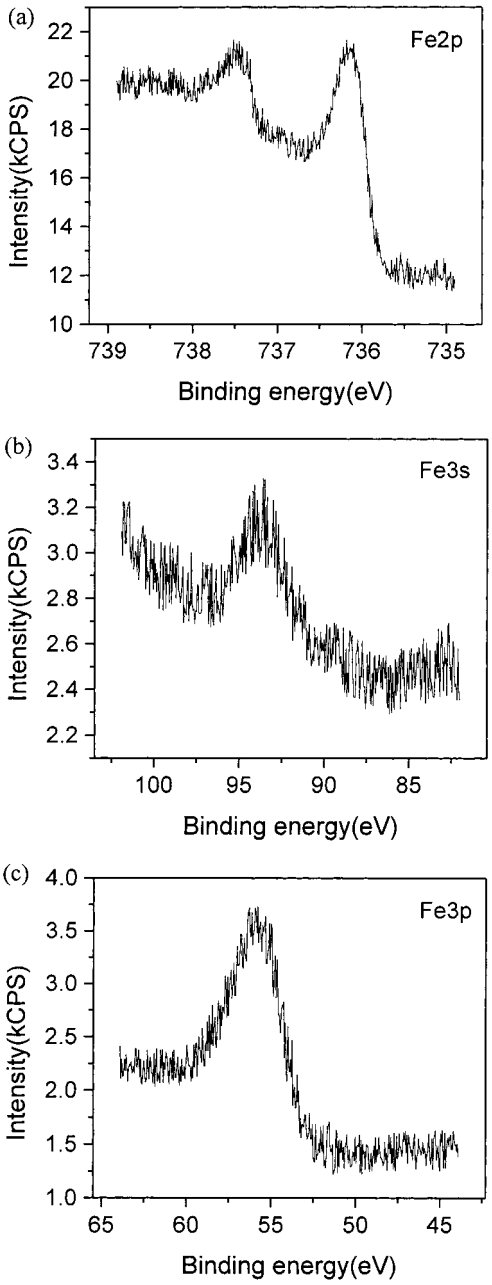

Figure 7. XPS spectra of Fe component in the nanoparticulate LB film (a, Fe 2p; b, Fe 3s; c, Fe 3p).

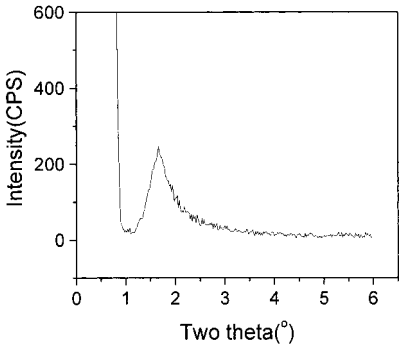

Figure 8. Small-angle X-ray diffraction of 8-layer Fe_2O_3 LB film on quartz substrate.

of the spectra is at about 600 nm. Because of the quantum size effect, this value is blue-shifted about 100 nm compared to Fe_2O_3 bulk powder.[15] There is a shoulder peak around 300 nm, which is the position of

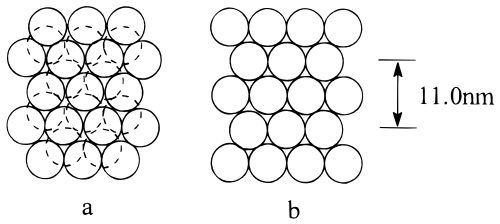

Figure 9. Schematics of Fe_2O_3 LB film (a, a top view of an Fe_2O_3 nanoparticle bilayer; b, a lateral view of the nanoparticulate LB film).

Table 1. Sensitivity of Fe_2O_3 LB Film to Alcohols at Different Concentrations

	concentration (ppm)			
	15	35	50	60
MeOH	2	2.1	4	16
EtOH	3.7	4.2	12	23
i-PrOH	1	6	20	100

the biexciton excitation of Fe_2O_3.[16] The inserted figure presents the plot of the absorbance at 300 nm as a function of the number of layers. The linear relationship between the absorption intensity and the number of layers suggests that the nanoparticulate films obtained from compression were well transferred onto the quartz substrate at a constant transfer ratio. It shows that every monolayer is rather uniform, which agrees with the results observed in Figure 5b.

Component Analysis of the LB Film. XPS is a useful method for obtaining the component and structural information on the thin film. Within the experimental limit, only the valence band of Fe and O atoms of 8-layer nanoparticulate LB film deposited on quartz substrate were detected, while Si 1s in the substrate was not detected. It further supports the above results that the nanoparticles are packed fairly closely in the film. The XPS spectra of Fe component in the film are shown in Figure 7. The electron binding energies of Fe 3s (93.6 eV), Fe 2p (711.3 eV), and Fe 3p (55.7 eV) all correspond to those of α-Fe_2O_3 and are different from those of α-FeOOH.[17−19] This result proves that the nanoparticles are well-crystallized as a corundum phase of α-Fe_2O_3. Compared to the theoretical ratio of Fe_2O_3, the molar ratio of O/Fe (19/7) is very large, indicating the high activity of the film surface. The excessive oxygen results from the adsorption of oxygen by the film surface in air.

Periodic Structure of α-Fe_2O_3 Nanoparticulate LB Film. Figure 8 is the small-angle X-ray diffraction pattern of an 8-layer nanoparticulate LB film deposited at 30 mN m^{-1} on quartz substrate. The Bragg peak at 1.66°, corresponding to (002) diffraction peak, indicates that the nanoparticulate LB film forms a perfect layer structure. According to the Bragg formula $2d \sin \theta = n\lambda$, in which θ is the Bragg angle, n the order of diffraction ($n = 2$), λ the wavelength of X-ray which equals 0.15405 nm, and d the spacing between two crystal faces, a long spacing of 11.0 nm is obtained. This value is close to one repeated at thr periodic length (10.7 nm), which is calculated by the hexagonal close-packed structure model with the average particle size of 6.2 nm. Therefore, we propose the schematic of an ideally periodic structure of α-Fe_2O_3 nanoparticulate LB film packing on the substrate, as illustrated in Figure 9. In brief, we suggest that the α-Fe_2O_3 nanoparticulate film built up by LB technique and colloid chemical method has a three-dimensional ordered structure.

Gas-Sensing Properties. Ferric oxide is a conventional gas-sensing material, which has been used for detecting the combustible gases. It is available on the market. We have determined the gas-sensing characteristics of this nanoparticulate LB film to alcohols at ambient temperature. From the measurement results, listed in Table 1, we see that the film can detect ethanol vapor down to 15 ppm, while reported Fe_2O_3 sensors could barely detect such low concentrations of C_2H_5OH (as well as other combustible gases) at room temperature. The ethanol detection limit of the Fe_2O_3 thin-film sensor[20] prepared by PCVD method was 200 ppm at the working temperature of 250 °C. The sintered sensor, made of ferric oxide nanopowder,[21] was sensitive to 5000 ppm of ethanol at atmosphere of 400 °C. Combination of LB technique with nanoparticles greatly improves the gas sensitivity of ceramic material at room temperature.

When the film is exposed to the same concentration of different alcohols, the sensitivity of the film increases with the length of the alkyl chain at concentrations higher than 35 ppm. The LB film shows faster responses to the tested gas. The response−recovery time to these alcohols is within 1 and 3 min, respectively. Good gas-sensing characteristics of this film at room temperature are possibly related to the high activity of the film surface resulting from the large O/Fe ratio and large ratio of surface area to bulk volume. Thus, it has potential application as a sensor for alcohols at ambient temperature.

Conclusion

Three-dimensional ordered α-Fe_2O_3 nanoparticulate film was constructed by the Langmuir−Blodgett technique and colloid chemical method. The nanoparticulate films could be formed on the surface of α-Fe_2O_3 hydrosol after aging of the sol or by compressing of the nanoparticles on the surface of the hydrosol. AFM and TEM studies indicate that the particles in the monolayer packed more closely and homogeneously with increasing aging time or surface pressure. The periodic structure of the LB film is obtained with a long spacing of 11.0 nm, suggesting that α-Fe_2O_3 nanoparticles pack as hexagonal close-packed structure. The LB film has good sensitivity to alcohols at room temperature, which is related to the high ratio of O/Fe on the surface of the film.

Acknowledgment. We thank Dr. Lixin Cao and Xu Wang for their help and discussion. This work was supported by National Natural Science Foundation of China (29633010) and Youth Foundation of Heilongjiang Province.

CM990690+

(15) Miyoshi, H.; Yoneyama, H. *J. Chem. Soc., Faraday Trans.* **1989**, *85*, 1873.
(16) Sherman, D. M.; Waite, T. D. *Am. Mineral.* **1985**, *70*, 1262.
(17) Mcintyre, N. S.; Zetaruk, D. G. *Anal. Chem.* **1977,** *49*, 1521.
(18) Welsh, I. D.; Sherwood, P. M. A. *Phys. Rev. B* **1989**, *40*, 6386.
(19) Peng, X. G.; Zhang, Y.; Yang, J.; Zou, B. S.; Xiao, L. Z.; Li, T. J. *J. Phys. Chem.* **1992**, *96*, 3412.
(20) Xu J. Q.; Shen Y. S., *Chem. Sens. (Chinese)* **1993**, *13* (2), 48.
(21) Nakatani, Y.; Matsuoka, M. *Jpn. J. Appl. Phys.* **1982**, *21*, L758.